ISCI, Volume *2*

Supplemental Information

YY1 Upregulates Checkpoint Receptors and Downregulates Type I Cytokines in Exhausted, Chronically Stimulated Human T Cells

Mumtaz Y. Balkhi, Gabor Wittmann, Fang Xiong, and Richard P. Junghans

Supplemental Information

Transparent Methods

Tissue and blood samples

Studies involving de-identified human samples were obtained after approval through the Tufts Health Science Campus Institutional Review Board (IRB). The malignant melanoma and normal healthy skin frozen sections were obtained from the Cooperative Human Tissue network (Philadelphia, PA). The purified peripheral blood mononuclear cells (PBMCs) from untreated ten HIV patients were obtained upon request from Retrovirus laboratory, University of Washington, Seattle, WA. Universal precautions were followed while working with the human samples.

Bioinformatics

The *IL2* promoter (GenBank and promoter database accession number, NM_000586 and 32233, respectively) and *YY1* promoter (GenBank and promoter database accession number, NM_003403 and 12193, respectively) were retrieved using the transcriptional regulatory element database (TRED) (https://cb.utdallas.edu/cgi-bin/TRED/tred.cgi?process=searchPromForm). The data on transcription factors binding to the consensus binding sequences were obtained through TRANSFAC database (www.gene-regulation.com). We used the "best selection criteria" for transcription factor binding sites to help minimize false positives.

Reporter plasmids, reporter assays and site directed mutagenesis

A human *IL2* promoter luciferase pGL3-NFAT plasmid (-326 to +46 bp) was a gift from Jerry Crabtree (Addgene plasmid #17870) (Clipstone and Crabtree, 1992; Northrop et al., 1994). The YY1 binding site, 5'-CCCCCATAAT-3', in the IL2 promoter luciferase was mutated to 5'-aaCaaAgAAc-3' using the service of GenScript Inc. (item cat. SC1622). Human YY1 promoter luciferase construct YY1-pGLuc-basic was a kind gift from Dr. Guangchao Sui of Wake Forest Health Sciences, NC (Balkhi et al., 2012). The cJun/ATF2 octameric palindrome cyclic AMP-response element (CRE), 5'-TGACGTCA-3', was mutated to 5'-cGgCaTaA-3' using the service of

GenScript Inc. (Item cat. 426354-1).

The reporter assays and plasmid overexpression were performed in 6 well tissue culture plates. $5x10^6$ T cells were transfected with plasmids using Amaxa human T cell nucleofector Kit, cat. VPA-1002 (Lonza). Transfections were performed using Amaxa nucleofector II device, program no. T-023/T-020. Luciferase assays were generally performed 48 hours after transfections. We ectopically express the *IL2* promoter construct in combination with a renilla lucifearse reporter to serve as an internal control and activity was measured using dual luciferase reporter assay system (Promega, cat. E1910). The YY1 promoter luciferase assay was measured from T cell culture supernatants using BioLux Gaussia lucferase assay kit (New England Biolabs, cat. no. E3300S). Amounts of transfected plasmids were kept proportionally constant. Samples were assayed for reporter activity using a Gloma 20/20 Luminometer (Promega), essentially using the recommended parameters provided by the reagent suppliers.

Antibodies, shRNA and inhibitors

The following antibodies were used for cell staining: PE-conjugated anti-human CD279 (PD-1) (cat. 12-2799), CD223 (LAG-3) (cat. 12-2239), Tim3 (cat. 12-3109), and CD3-PECyanine7 (cat. 25003182), all of which were purchased from eBioscience, and FITC-conjugated anti-human CD8 (Invitrogen) and CD4 (BD Biosciences, cat. 340133). Pacific Blue-conjugated PD1 (cat. 329920), PE-conjugated PD-L1 (cat. 329705) and purified PD-L1 (cat. 329702) was purchased from BioLegend. In addition, PE-conjugated (cat. 555783, Pharmingen) was used as an isotype control. T cell apoptosis was detected through flow cytometric analysis using the FITC Annexin V apoptosis detection kit I (BD Pharmingen, cat. 556547) in conjunction with the vital dye, propidium iodide (BD Pharmingen, cat. 51-66211E). In addition, following antibodies were used in westerns, phospho-MKK3$^{(Ser189)}$/MKK6$^{(Ser207)}$ (cat. 12280), phospho-SEK1/MKK4$^{(Ser257/Thr261)}$ (cat. 9156), MKK3 (cat. 5674), SEK1/MKK4 (cat. 9152BC), p38-alpha MAPK (cat. 9217BC), phospho-p38 MAPK$^{(T180/Y182)}$ (cat. 4511BC), ZAP-70 (cat. 2709BC), phospho-ZAP-70$^{(Y319)}$/Syk$^{(Y352)}$ (cat. 2701BC), AKT (cat. 9272), phospho-AKT$^{(S473)}$ (cat. 9271), p44/42 MAPK (Erk1/2) (cat. 9102), phospho-p44/42 MAPK

(Erk1/2)$^{(Thr202/Tyr204)}$ (cat. 9106) and β-actin (cat. 4970S), all of which were purchased from Cell Signaling, and anti-Ezh2 (cat. 07-689), anti-YY1 (cat. AB10007), anti-phospho-ATF2$^{(Thr\ 69/71)}$ (cat. 05-891) and anti-ATF2 (cat. 04-1021), all of which were purchased from Millipore. We also used Anti-cJun (BD, cat. 610326) and phospho-c-Jun$^{(Ser\ 63/73)}$ antibodies (Santa Cruz, cat. sc16312). The human IL2 neutralizing antibody was purchased from R & D Systems (cat. AF-202-NA). An anti-p38α MAP Kinase$^{(Tyr\text{-}323)}$ (cat. PP3411) was acquired from ECM Biosciences. The human YY1 specific shRNA (cat. sc-36863) and control shRNA plasmid (sc-108060) were obtained from SantaCruz Biotechnology.

In experiments using p38MAPK, JNK, MEK1 and Ezh2 inhibitors, cells were grown in the continued presence of inhibitors. After each wash and activation step, cells were treated with a fresh batch of inhibitors. The following inhibitors were used: MAPKp38-SB202190 (10μmol/ml) (Sigma, cat. S7067), JNK-SP600125 (10μmol/ml) (Sigma, cat. S5567), MEK1-PD98059 (5μmol/ml) (Calbiochem, cat. 513001), MEK1/2-inhibitor III (5μmol/ml) (Calbiochem, cat. 444966) and Ezh2-UNC999 (10 nmol) (Millipore, cat. 505052). DMSO was used as a mock treatment. The specificity of p38MAPK, JNK and MEK1 inhibitors to block the downstream kinases, phospho-ATF2, phospho-cJun and phospho-ERK, respectively, was confirmed by westerns (Figure S10A). The continued presence of p38MAPK/JNK/MEK1 inhibitors in T cell culture did not produce noticeable toxicity (Figure S10B).

Westerns, Native gels and Co-immunoprecipitations

For denaturing westerns, 20–40 μg of protein extracted from T cells was used. RIPA lysis buffer (Sigma, cat. R0278) was used to prepare whole cell extracts. For native gel analysis, cells were lysed in native lysis buffer (50mM Tris-Cl, pH 8.0; 1% NP40; 150mM NaCl, 100μg leupeptin, 1mM PMSF, 5mM orthovanadate). For both native and denaturating conditions, samples were resolved on 4-15% TGX precast gels (Bio-Rad, cat. 456-1084) with the difference in running buffer. Native samples were run without SDS. Generally, 10μg of protein extract dissolved in 2x Native PAGE sample buffer (Bio-Rad, cat. 161-0738) was run on the gel following the

procedures described previously (Balkhi et al., 2010). For Co-IPs, CD8 enriched T cells were stimulated repeatedly *in vitro* and lysed in a standard Co-IP lysis buffer, and then 500µg of whole cell extract was prepared and incubated with YY1 antibody pre-absorbed to Protein A/G Agarose (Santa Cruz Biotechnology, cat. sc-2003). Western transfers were performed on Immobilon transfer membranes (Millipore, cat. IPVH08100). Membranes were blocked for 1 hr at RT in TBS-T buffer containing 5% dry skim milk powder and then incubated overnight in primary antibody. Membranes were washed 3 times in TBST-milk and incubated for 1 hr in anti-mouse or anti-rabbit IgG-HRP antibodies (GE Healthcare, cat. NA931 and NA934). After secondary antibody incubation, membranes were thoroughly washed for 2 hours. Immuno-detection was performed using chemiluminescence substrate reagents (Perkin Elmer) and autoradiography detection on HyBlot CL film (Denville Scientific). Membrane stripping was performed with Restore Western blot stripping buffer (Thermo Fisher Scientific, cat. 21059). The immunoprecipitation and westerns were performed with antibodies derived from different species to avoid cross reactivity.

Chromatin immunoprecipitation and Electrophoretic mobility shift assay (EMSA)

Chromatin immunoprecipitation assay. The ChIP assay was performed using a ChIP-IT high sensitivity kit (Active Motif, cat. 53040), following the manufacturer's recommended protocol. Human CD4+ T cells were repeatedly activated with CD3/CD28 beads in the continued presence of Ezh2 inhibitor or transfected with YY1 shRNA and a control after 2nd stimulation. Approximately, 15µg of chromatin was used in each reaction with an antibody that specifically recognizes H3K27me3 (Active Motif, cat. 39155). Fold enrichment was calculated relative to IgG and input. We used the primer pair that amplifies the *IL2* promoter sequence containing the YY1 binding site: F-5'-CATCAGAAGAGGAAAAATGAAGGT-3', R-5'-TCTTGAACAAGAGATGCAATTTAT-3'.

EMSA was performed using LightShift chemiluminescent EMSA kit (Thermo Scientific, cat. 20148). We followed the manufacturer's procedure to perform the assay. The primer duplex

containing the cJun/ATF2 octameric palindrome cyclic AMP-response element (CRE) present on the *YY1* promoter was modified with biotin at the 5' end. We used the following primer duplex:

5'Biotin- GGCGGTGGCGGCGGCGGCGGCGCGCTGACGTCACGCG-3'

3'-CGCGCGACTGCAGTGCGC-Biotin 5'

In addition, we used a non-specific biotin modified probe provided by the manufacturer. We used 10µg of nuclear extract obtained from the activated T cells in the binding reaction. All the reaction components, phospho-cJun and ATF2 were added in the order recommended by the manufacturer. Gels were run in 0.5X TBE using 4-15% precast polyacrylamide gels, subsequently gels were transferred onto a positively charged nylon membrane (Hybond-N+, Amersham pharmacia biotech) in 0.5X TBE. After the transfer membrane was crosslink for 10-15 minutes using UV transilluminator (Fisher Scientific). Protein binding to the biotin-labeled DNA was detected through chemiluminescence method as described by the manufacturer. To detect phospho-cJun and phospho-ATF2 binding to the probe, we incubated membrane first with secondary rabbit HRP antibody. The same membrane was stripped and reprobed with secondary mouse HRP. DNA oligonucleotides were acquired from Sigma. Each time EMSA was performed, we included a complete set of three control reactions provided by the supplier.

Immunohistochemistry and immunofluorescence

Formalin-fixed paraffin tissue samples of human metastatic melanoma were cut at 4 µm sections and placed on positively-charged slides. Slides were subsequently incubated in a 60^{o} C oven for 1 hour, cooled, and deparaffinized. Rehydration of slides was performed in graded ethanol solutions. Antigen retrieval was performed by the Heat-Induced Epitope Retrieval procedure. In this procedure slides were first placed in a IX solution of Target Retrieval Solution (Dako, pH 6) for 25 min at 96˚C using a vegetable steamer (Black and Decker) and cooled for 20 min. Endogenous peroxidase was blocked by incubating the slides in 3% hydrogen peroxide aqueous solution and 10% goat serum. Sections were then sequentially stained, first with mouse anti-CD3 (Santa Cruz, sc-1239) for 60 min. then with HRP goat anti-mouse polymer

secondary antibody (Vector) for 30 min. The chromogen used was 3,3´-diaminobenzidine (DAB+, Vector Labs). Rabbit anti-YY1 (Abcam, cat. ab109237) and rabbit anti-Ezh2 (Novus Biological, cat. NBP2-38143) was subsequently applied, followed by secondary biotinyated goat anti-rabbit. ABC alkaline phosphatase was used for the YY1 and Vector Red was a chromogen. A negative control consisted of omitting the primary antibody.

For IF, the fresh-frozen mounted sections were fixed with methanol at −20 °C for 5 min. Sections were permeabilized with 0.25% Triton-X-100 for 20 min, and then blocked with 2% normal horse serum in PBS for 20 min. Sections were incubated overnight in a cocktail of primary antisera of CD3/PD1 and CD3/phospho-cJun for dual immunofluorescence. The primary antibodies used were mouse anti-PD1 (cat. ab52587), goat anti-CD3 (Santa Cruz, cat. sc-1127), and rabbit ant-phospho-cJun$^{(Ser63/73)}$ (Santa Cruz, cat. sc-16312-R). Subsequent detections were performed with a mixture of secondary antibodies consisting of Cy3-conjugated donkey anti-rabbit IgG (Jackson Immunoresearch, 1:200), Alexa 488-conjugated donkey anti-mouse IgG (Jackson), and Cy3-conjugated donkey anti-sheep IgG (Jackson). Images were captured with a Carl Zeiss Axioskop fluorescence microscope (Axioskop 40; Carl Zeiss Inc.)

_q_RT-PCR and ELISA

Total RNA was extracted from T cells using Trizol Reagent (Life Technologies). Reverse transcription reactions were performed using M-MuLV reverse transcriptase (New England Biolabs, cat. M0253L). *q*PCR amplification reactions were performed using SYBR GREEN PCR master mix (applied biosystems). The following primers were used in the qPCR amplification reactions: IL2, F-5'-AACTCCTGTCTTGCATTGCAC-3', R-5-' GCTCCAGTTGTAGCTGTGTTT-3'; IFNγ, F-5'-TCGGTAACTGACTTGAATGTCCA-3', R-5'-TCGCTTCCCTGTTTTAGCTGC-3'; YY1, F-5'-ACGGCTTCGAGGATCAGATTC-3', R-5'-TGACCAGCGTTTGTTCAATGT-3'; GAPDH, F-5'-ACAACTTTGGTATCGTGGAAGG-3', R-5'-GCCATCACGCCACAGTTTC-3' Gene amplification reactions were performed with iCycler 480 (Roche). Fold changes were calculated using the LightCycler software basic relative quantitation method (ΔΔcp). $\Delta\Delta cp_{\text{(Fold Change)}} = \Delta cp\ \text{Target}_{\text{(Gene)}} -$

Δcp Calibrator $_{(GAPDH)}$.

ELISA assays were performed using human IL2 and IFNγ Ready-SET-Go kits (eBioscience). We included three replicates for each experimental set and each experiment was repeated three or more times. ELISA was performed on the supernatant saved from each stimulation step. CD4+ or CD8+ T cells were stimulated with anti-CD3/CD28 beads and cultured for 48 hours, after which cells were spun down and supernatants carefully removed and saved at -20^{o}C. The same procedure was followed for the rest of the stimulation steps.

Cell culture and Flow cytometry

Human T cell isolation and culture *in vitro*. CD4+ and CD8+ T cells were enriched from peripheral blood mononuclear cells obtained from healthy donors. We received leukoreduction filters from Boston Children's Hospital that were processed using histopaque (Sigma) cushions to separate PBMCs. Human CD8+ and CD4+ cells were enriched using naïve CD8 and CD4 T cell enrichment cocktail (BD Biosciences, cat. 51-900481 and 9002314, respectively). Approximately, 1x10^{6} T cells were initially plated in 24 well plates suspended in AIM-V medium (Life Technologies, cat. 12055-083), 5% heat inactivated human serum (Sigma, cat. F4135) without IL2 unless stated. IL2 when included in the growth medium was used at concentration of 300IU/ml (Chiron). Cells were stimulated the same day with T-Activator CD3/CD28 dynabeads (Life Technologies, cat. 11131D) following the manufacturer's recommendations. 48 hours after the first stimulation, cells were counted and washed, and beads were removed using a magnet. This was followed by a second, third and fourth round of stimulations with fresh batches of CD3/CD28 beads. In each stimulation step, the amount of beads used and the number of viable cells activated were kept proportionally equal. In the experiments requiring selective activations with anti-CD3 or anti-CD28 antibody alone, we used immobilized anti-OKT3 or anti-CD28 antibodies at a concentration of 1µg/ml.

Intracellular staining of T cells for flow cytometry analysis was performed using intracellular fixation and permeabilization buffer set (eBioscience, cat. 88882400). Briefly, T cells were incubated first with fluorescent conjugated surface antibodies for 40 minutes in FACS buffer. This

followed a onetime wash. Cells were then fixed with 100µl fixation buffer for 30 minutes followed by washes to remove fixation buffer. After the washes, cells were incubated for additional 30 minutes in 1X permeabilization buffer containing either anti-YY1 (Alexa 488) (abcam, cat. 199814) or anti-Ezh2 (Alexa 647) (BD Biosciences, cat. 563491), followed by two time washes in permeabilization buffer before flow cytometry analysis.

Flow cytometry of stained PBMCs and cultured T cells was performed with a multicolor BD LSR II at the Tufts University School of Medicine flow cytometry core. Analyses were performed with Flow Jo software. Samples with intracellular staining were gated on the well-permeabilized fraction.

CEA-CAR T cells and retroviral transduction

To produce second generation CEA-CAR T cells, T cells are modified by retroviral gene therapy to express a single chain antibody domain (sFv) that recognizes CEA tumor antigen. This anti-CEA binding domain is fused together with the full length sequence of CD28 co-stimulatory molecule and sequences of the ζ signaling chain of the CD3 complex (signal 1+2) (Figure 6A) (Nolan et al., 1999). The clinical grade CEA-CAR vector producing cells have been sucessfully tested in a number of *in vitro* studies as well as in a clinical setting to modify T cells for breast cancer clinical trials (Katz et al., 2015). The first generation CEA-CAR contains anti-CEA binding domain fused with ζ signaling chain (signal 1) (Nolan et al., 1999). Transduction of T cells with anti CEA-CAR vector were as previously described (Beaudoin et al., 2008).

MIP101 and MIPCEA, tumor cell coculture with CEA-CAR modified T cells. MIP101 is a CEA- undifferentiated human carcinoma cell line derived from liver metastases of colonic adenocarcinoma patients. The MIPCEA cell line was generated by stably expressing the full length *CEA* gene in MIP101 cells (Thomas et al., 1995). All cell lines tested negative for mycoplasma contamination using mycoplasma detection kit (Sigma, cat. D9307). Their coculture with CAR-T cells was performed in 12 well tissue culture plates. Approximately $3x10^5$ tumor cells were plated overnight prior to coculture. The next day, cells were treated with Mitomycin C (Millipore, cat.

475820) for 1 hr, following which cells were carefully washed three times. This was followed by their coculure with CAR -T cells in a 1:1 ratio either in the absence or presence of 10nm Ezh2 inhibitor (Millipore, cat. 505052) (Konze et al., 2013). Ezh2 inhibitor treatment was performed by incubating CAR-T cells with the inhibitor for 1 hour, after which CAR-T cells were put in coculture with the tumor cells. After 48 hours of coculture, CAR-T cells were recovered from culture, washed and exposed to a second batch of Mitomycin C treated tumor cells either in the absence or presence of 10nm Ezh2 inhibitor for an additional 48 hours. Modified T cells were again recovered, washed and exposed to a third batch of Mitomycin C treated tumor cells either in the absence or presence 10nm Ezh2 inhibitor for an additional 48 hours. Each time after the coculture, tumor cells were trypsinized (cellgro) and counted. In experiments requiring blocking of PD1 (nivolumab) or PD-L1 in MIPCEA and MIP101 cells, we used 20μg and 5μg respectively of clinical grade anti-PD1 antibody (courtesy Tufts Medical Center, Cancer Center) and purified anti-PD-L1 antibody (cat. 329702).

Statistical analysis

Data are presented as averages ± SD. Student's t-test was applied to perform pair-wise comparisons between different treatment groups or between control and treatment groups. *P* values less than 0.05 were considered statistically significant.

Figure S1
Balkhi et al.

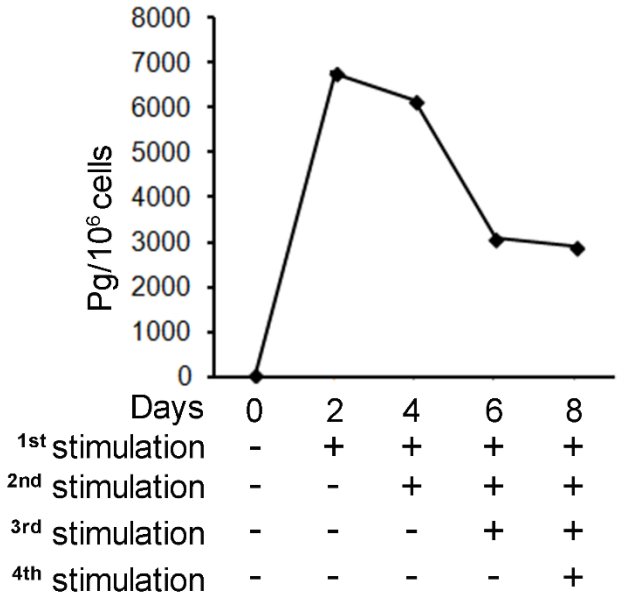

Figure S1. IFNγ production declines after repeated stimulations, (Related to Figure 1). ELISA for IFNγ production in CD4 T cells repeatedly stimulated in the presence of IL2.

Figure S2
Balkhi et al.

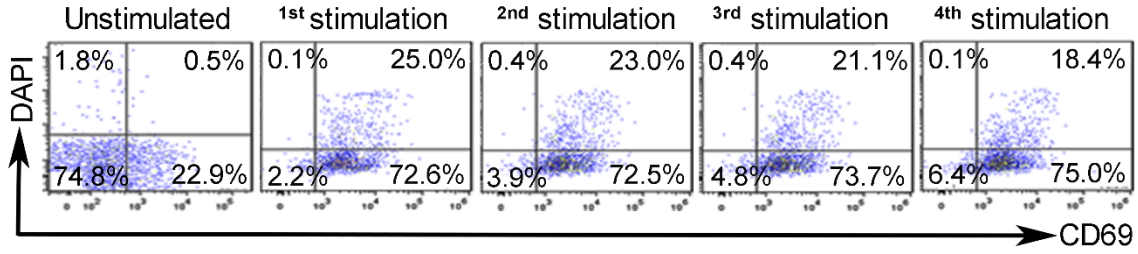

Figure S2. Exhausted T cells maintain activation status and viability after repeat stimulation, (Related to Figure 1). Flow cytometry analysis for CD69 activation marker in CD4 T cells after repeat stimulations. DAPI positive cells indicate percent dead cells. Viability was 75% or greater and CD69 was strongly positive throughout.

Figure S3
Balkhi et al.

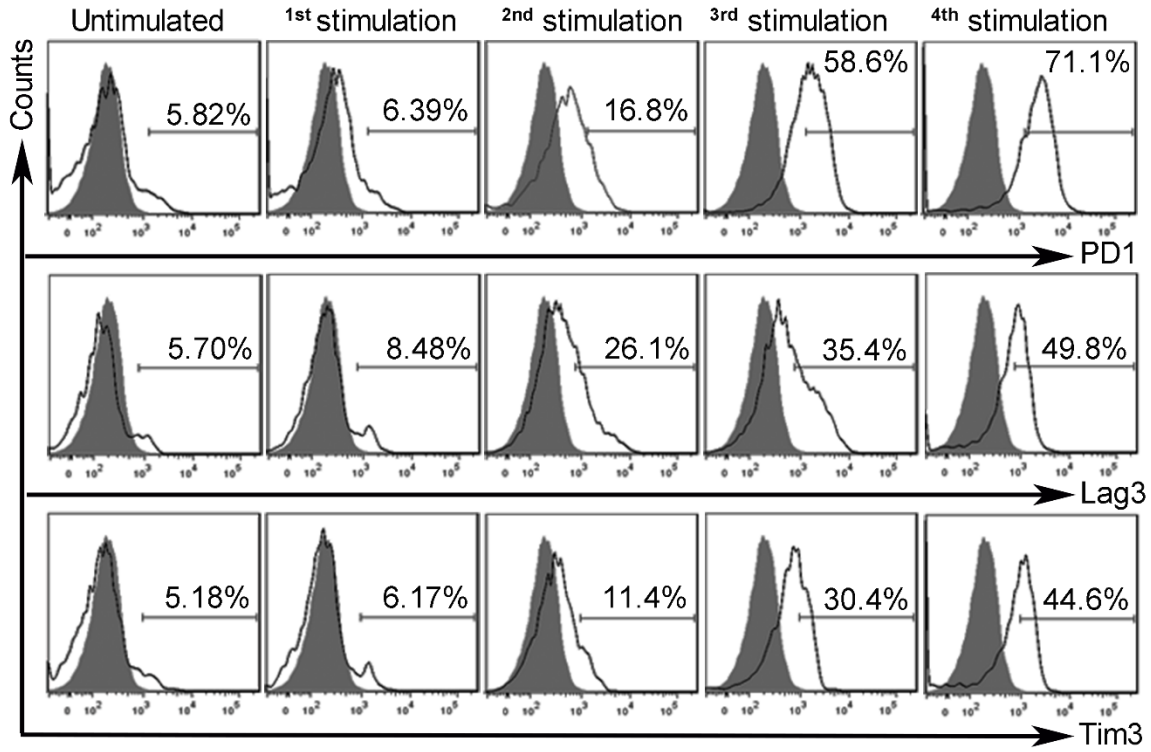

Figure S3. IL2 supplementation does not block exhaustion marker progression, (Related to Figure 1). Flow cytometry analysis showing expression of PD1, Lag3 and Tim3 in CD4 T cells repeatedly stimulated with anti-CD3/CD28 beads in presence of 300 IU/ml IL2.

Figure S4
Balkhi et al.

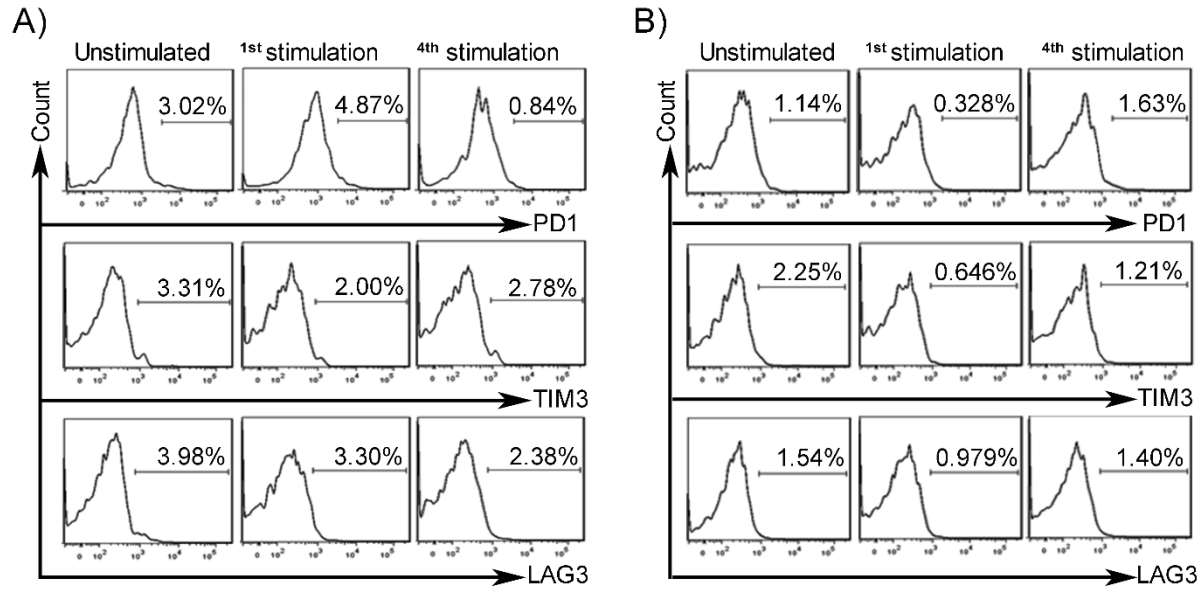

Figure S4. Persistent activation of T cells with signal 1 or signal 2 alone does not induce exhaustion phenotype, (Related to Figure 1). (A-B) FACS for exhaustion markers after repeat stimulation of CD4 T cells with immobilized (A) anti-CD3 or (B) anti-CD28 antibody on tissue culture plates. Unstimulated CD4 T cells were used as control.

Figure S5
Balkhi et al.

Figure S5. *IL2* promoter contains YY1 binding site, (Related to Figure 1). *IL2* promoter sequence showing putative transcription factor binding sites. YY1 binding site is close to HMG1, TFIID and ATG**.**

Figure S6
Balkhi et al.

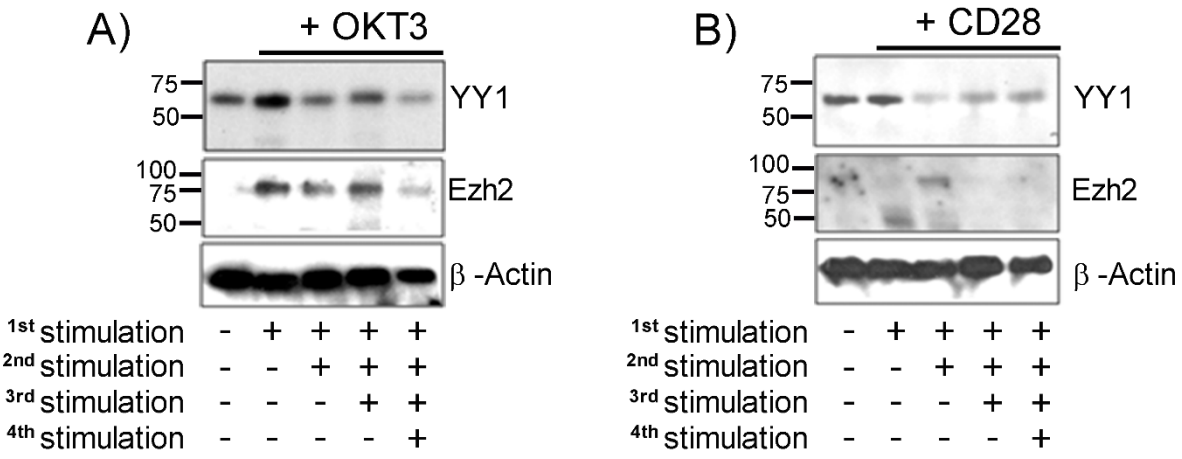

Figure S6. Persistent activation of T cells with signal 1 or signal 2 alone does not increase YY1 or Ezh2, (Related to Figure 2). Western blot of YY1 and Ezh2 protein in CD4 T cells that were repeatedly stimulated with immobilized (A) anti-CD3 antibody or (B) anti-CD28 antibody. β-actin was loading control.

Figure S7
Balkhi et al.

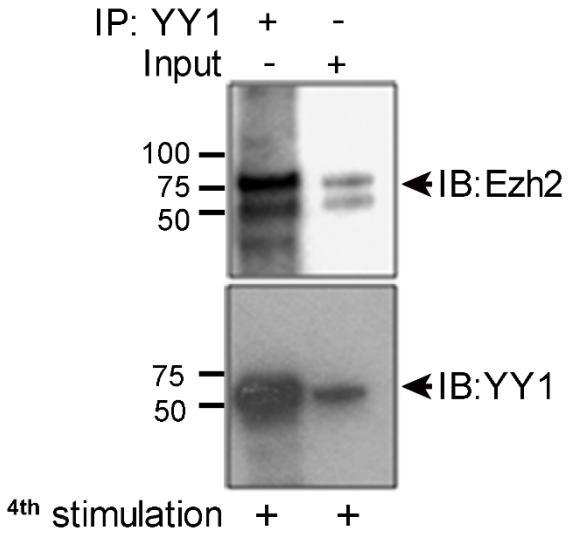

Figure S7. YY1 interacts with Ezh2 in exhausted T cells, (Related to Figure 2). Whole cell extracts were prepared after 4th stimulation of T cells and subjected to immunoprecipitation using anti-YY1 antibody followed by westerns with Ezh2. The same blot was reprobed with YY1 to demonstrate its precipitation.

Figure S8
Balkhi et al.

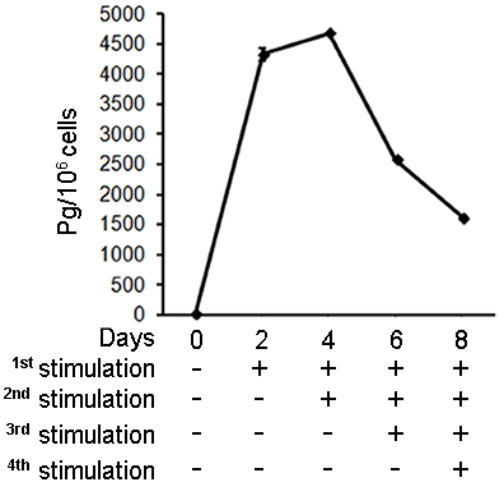

Figure S8. Ezh2 inhibitor does not protect against IFNγ shutdown. (Related to Figure 2). ELISA showing IFNγ production after repeated stimulations in the continued presence of Ezh2 inhibitor, compare with Figure S1.

Figure S9
Balkhi et al.

A)

PD1 Promoter

YY1 site

Matrix	Factor name	Position (strand)	Core score	Matrix score	Sequence
V$YY1_Q4_01	YY1	207 (+)	1.000	0.989	ccgtaaAATGGgggc
V$YY1_Q6_03	YY1	211 (-)	1.000	1.000	aaAATGG
V$MAF_Q6_01	MAF	254 (+)	1.000	0.964	tgcggAGTCAt
V$MAF_Q4	MAF	255 (+)	1.000	0.968	gcggAGTCAt
V$CJUN_Q6	C-Jun	258 (-)	1.000	1.000	gAGTCA
V$STAT3_01	STAT3	291 (-)	0.908	0.824	tggcaggtccgGGAAGtggag

B)

LAG3 Promoter

YY1 site

Matrix	Factor name	Position (strand)	Core score	Matrix score	Sequence
V$NFAT1_Q4	NF-AT1	23 (+)	1.000	1.000	GGAAAa
V$BLIMP1_03	Blimp-1	61 (-)	1.000	0.873	tgTCCAAtacag
V$XBP1_01	XBP-1	74 (-)	1.000	0.883	gcttagCACGTaatgaa
V$OCT1_03	Oct-1	80 (+)	1.000	0.994	cacGTAATgaagc
V$TCF1_Q5	TCF-1	124 (-)	1.000	1.000	aCAAAG
V$YY1_Q6_03	YY1	154 (+)	1.000	1.000	CCATTtt
V$ETS_B	c-Ets	172 (-)	1.000	0.935	taaggcTTCCTgtc

C)

TIM3 Promoter

GATA3 site

Matrix	Factor name	Position (strand)	Core score	Matrix score	Sequence
V$GATA3_Q4	GATA-3	12 (-)	1.000	1.000	tTATCT
V$HMGIY_Q3	HMGIY	18 (+)	1.000	0.939	aatacAATTTtctca
V$CEBPG_Q6	C/EBPgamma	29 (+)	0.845	0.904	ctcATTTTataaa
V$POU6F1_01	POU6F1	37 (-)	1.000	0.894	ATAAAttatat
V$CETS1_Q6	C-ets-1	190 (-)	1.000	1.000	aCTTCCt
V$SPI1_04	SPI1	190 (-)	1.000	1.000	acTTCCT
V$ELF1_Q5	Elf-1	191 (-)	1.000	1.000	cTTCCT
V$SPI1_Q5	SPI1	191 (-)	1.000	1.000	cTTCCT

D)

YY1 Promoter

cJun/ATF2

Matrix	Factor name	Position (strand)	Core score	Matrix score	Sequence
V$PAX4_01	Pax-4	310 (-)	0.881	0.843	ccgcccacccgCCTCAacccc
V$CREBP1_Q2	CRE-BP1	555 (+)	1.000	0.972	gcTGACGtcacg
V$CREB_01	CREB	557 (+)	1.000	1.000	TGACGtca
V$CREB_01	CREB	557 (-)	1.000	1.000	tgaCGTCA
V$CREBP1CJUN_01	CRE-BP1/c-Jun	557 (+)	1.000	1.000	tGACGTca
V$CREBP1CJUN_01	CRE-BP1/c-Jun	557 (-)	1.000	1.000	tgACGTCa
V$PAX4_01	Pax-4	557 (+)	0.977	0.897	tgacgTCACGcgccgcgggcc
V$CDPCR1_01	CDP CR1	672 (-)	1.000	0.930	cagaTCGATt

E)

Gene	Transcription Factor	Position from TSS
IL2	YY1	-5
IFNγ	YY1/AP1	-198/-189
PD1	YY1	-433
LAG3	YY1	-492
TIM3	GATA3/YY1	-633
YY1	cJun/ATF2	-136
Ezh2	cJun	5

Figure S9. Transcription factor consensus sites in exhaustion related promoters, (Related to Figure 3). (A-D) Promoter sequences match in Transfac database (Biobase) for TF binding sites using cutoffs to minimize false positive matches. Consensus sites are shown in *PD1*, *Lag3*, *Tim3 and YY1* promoters along with scores. Promoter sequences were retrieved using the transcriptional regulatory element database (TRED) (https://cb.utdallas.edu/cgi-bin/TRED/tred.cgi?process=searchPromForm). Capital letters in the matching sequence indicate positions of the core strings. **(E)** Table shows distance of key TF binding sites from respective transcription start sites (TSS).

Figure S10
Balkhi et al.

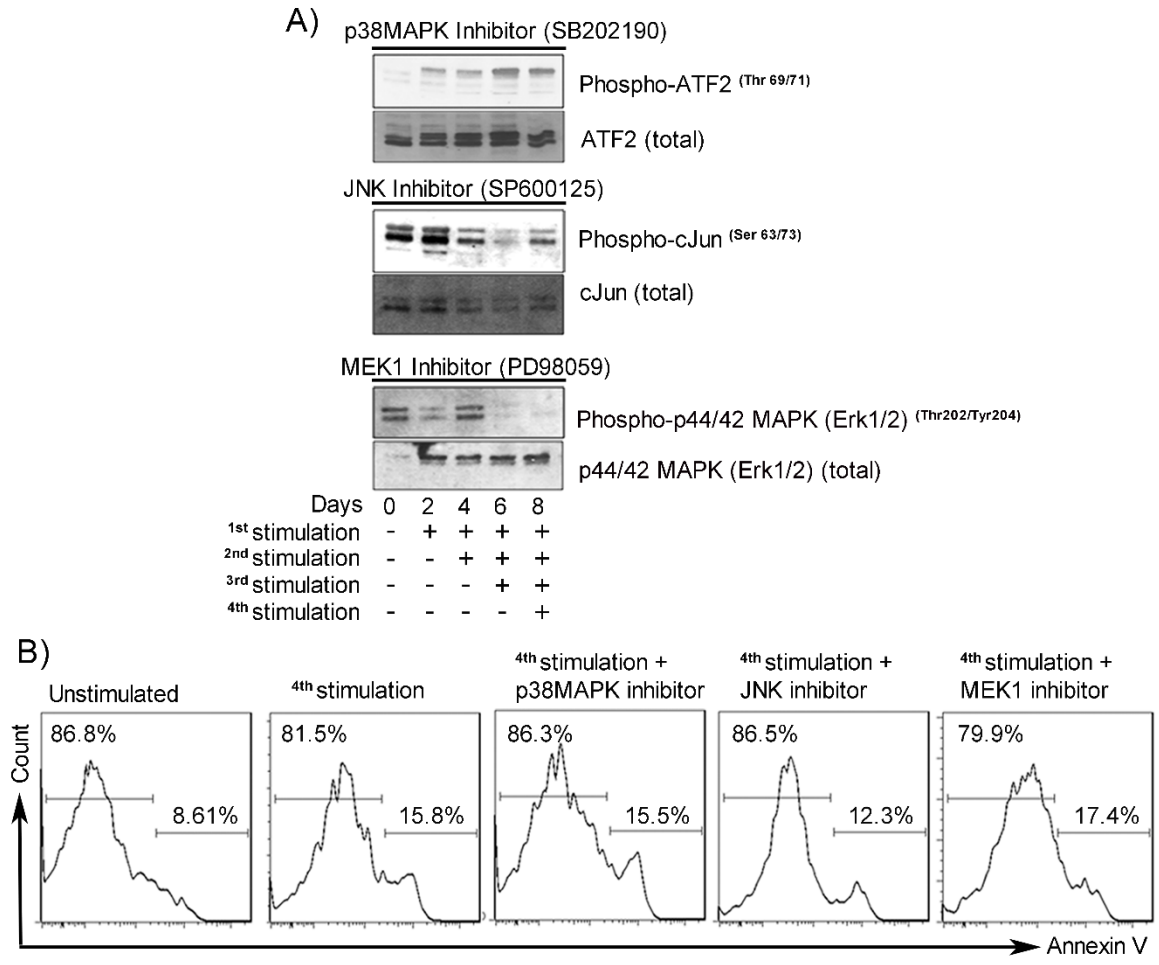

Figure S10. Targeted inhibition of p38MAPK/JNK signaling pathways, (Related to Figure 5). (A) Kinase activities by western blot**.** CD8+ T cells were repeatedly stimulated with anti-CD3/CD28 beads in continued presence of inhibitors targeting p38MAPK, JNK or MEK1 (methods). Westerns show effect of inhibitors on the p38MAPK, JNK and MEK1 kinase targets: phospho-ATF2, phospho-cJun and Phopho-ERK1/2, respectively, which are all substantially below control levels (compare with Figure 4D). **(B)** Viability by Annexin V staining. As a control on nonspecific toxicity, CD8+ T cells in (A) were stained with Annexin V after the 4th stimulation and analyzed by FACS for cellular apoptosis. Viability of >80% was maintained in all cultures.

Figure S11
Balkhi et al.

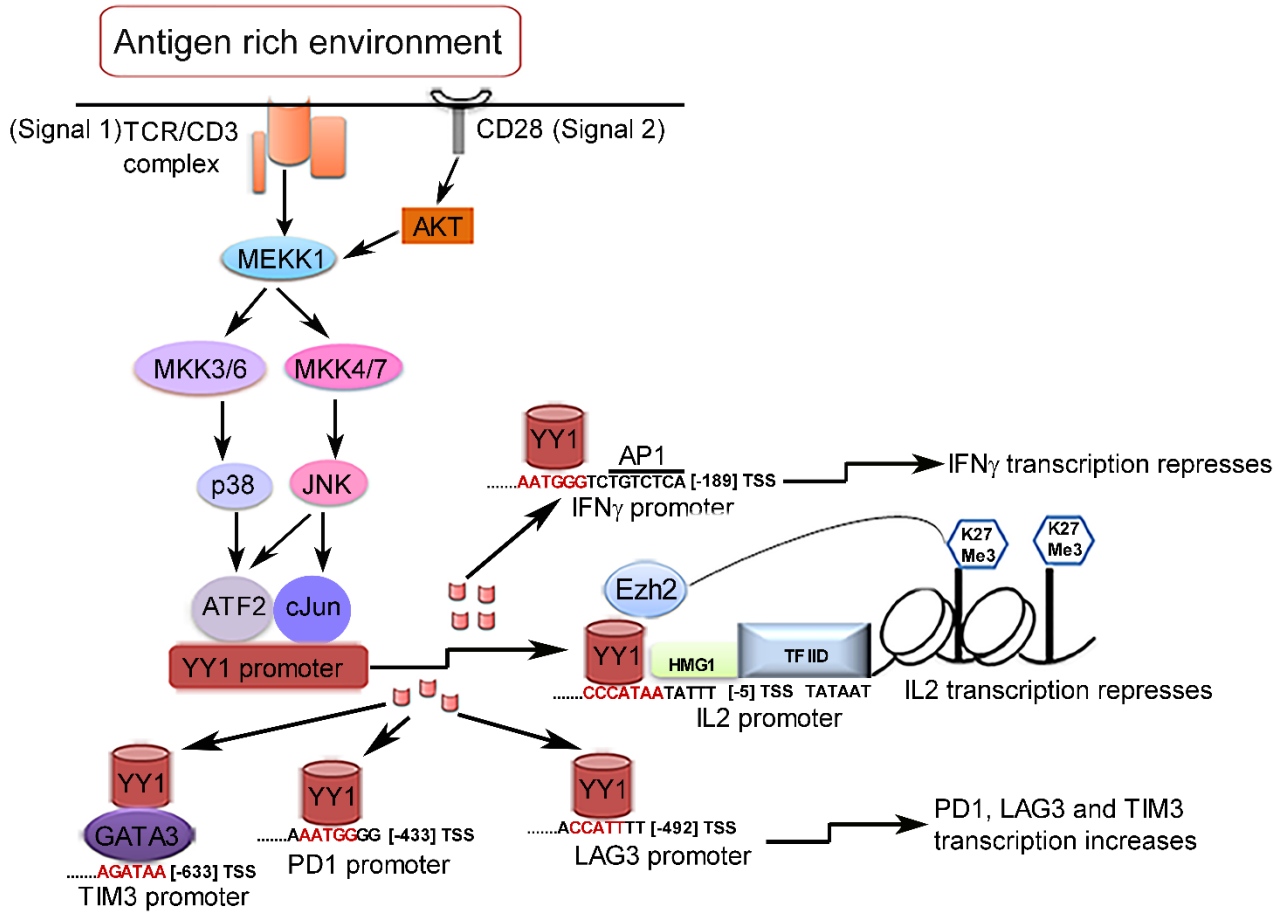

Figure S11. Summary diagram of exhaustion regulation, (Related to Figure 5).

Figure S12
Balkhi et al.

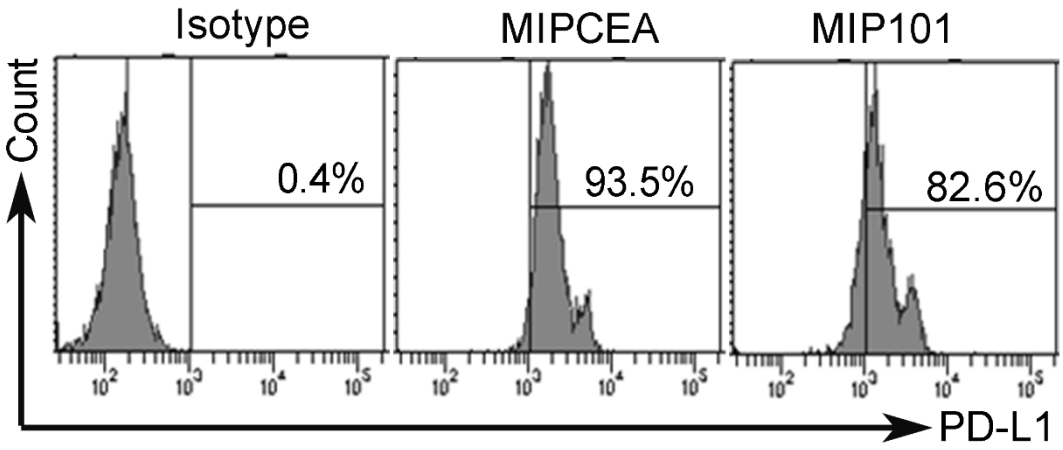

Figure S12. MIPCEA and MIP101 tumor are positive for PDL1, (Related to Figure 6). FACS analysis showing PDL1 expression on MIPCEA and MIP101 epithelial cancer cell lines.

Figure S13
Balkhi et al.

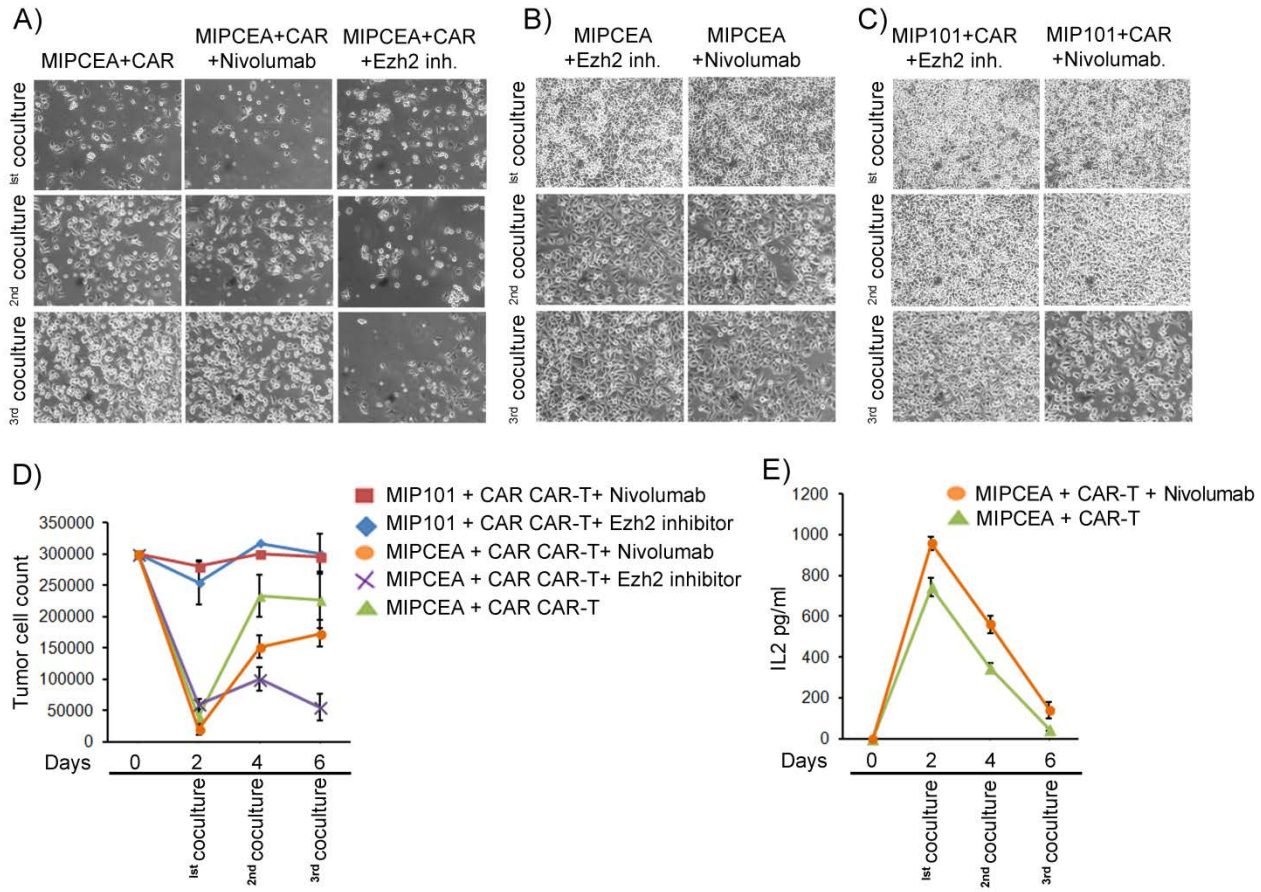

Figure S13. Rescue from cytotoxic exhaustion with nivolumab compared to Ezh2, (Related to Figure 6). (A) 2nd generation CAR-T cells with ~50% modification were cocultured 3 times for two days with MIPCEA cell line either in continued presence of nivolumab (20µg/ml) or Ezh2 inhibitor (10nm) or no additive and imaged. **(B)** MPI-CEA cell line incubated with inhibitors alone showed no toxicity.**(C)** Antigen-negative MIP101 cells were not killed by CAR-T cells in presence of exhaustion inhibitors. **(D)** Cell counts obtained from experiment in (A-C), showing partial rescue of killing effect with nivolumab and more complete rescue witth Ezh2 inhibitor. Three replicates per assay; representative of three experiments. **(E)** IL2 ELISA shows high initial IL2 production in MIPCEA/CAR-T cell cocultures in presence or absence of nivolumab that declined in parallel when CAR T cells were re-exposed to second and third batches of target tumor cells.

Supplemental References:

Balkhi, M.Y., Fitzgerald, K.A., and Pitha, P.M. (2010). IKKalpha negatively regulates IRF-5 function in a MyD88-TRAF6 pathway. Cell Signal *22*, 117-127.

Balkhi, M.Y., Willette-Brown, J., Zhu, F., Chen, Z., Liu, S., Guttridge, D.C., Karin, M., and Hu, Y. (2012). IKKalpha-mediated signaling circuitry regulates early B lymphopoiesis during hematopoiesis. Blood *119*, 5467-5477.

Beaudoin, E.L., Bais, A.J., and Junghans, R.P. (2008). Sorting vector producer cells for high transgene expression increases retroviral titer. J Virol Methods *148*, 253-259.

Clipstone, N.A., and Crabtree, G.R. (1992). Identification of calcineurin as a key signalling enzyme in T-lymphocyte activation. Nature *357*, 695-697.

Katz, S.C., Burga, R.A., McCormack, E., Wang, L.J., Mooring, W., Point, G.R., Khare, P.D., Thorn, M., Ma, Q., Stainken, B.F.*, et al.* (2015). Phase I Hepatic Immunotherapy for Metastases Study of Intra-Arterial Chimeric Antigen Receptor-Modified T-cell Therapy for CEA+ Liver Metastases. Clin Cancer Res *21*, 3149-3159.

Konze, K.D., Ma, A., Li, F., Barsyte-Lovejoy, D., Parton, T., Macnevin, C.J., Liu, F., Gao, C., Huang, X.P., Kuznetsova, E.*, et al.* (2013). An orally bioavailable chemical probe of the Lysine Methyltransferases EZH2 and EZH1. ACS Chem Biol *8*, 1324-1334.

Nolan, K.F., Yun, C.O., Akamatsu, Y., Murphy, J.C., Leung, S.O., Beecham, E.J., and Junghans, R.P. (1999). Bypassing immunization: optimized design of "designer T cells" against carcinoembryonic antigen (CEA)-expressing tumors, and lack of suppression by soluble CEA. Clin Cancer Res *5*, 3928-3941.

Northrop, J.P., Ho, S.N., Chen, L., Thomas, D.J., Timmerman, L.A., Nolan, G.P., Admon, A., and Crabtree, G.R. (1994). NF-AT components define a family of transcription factors targeted in T-cell activation. Nature *369*, 497-502.

Thomas, P., Gangopadhyay, A., Steele, G., Jr., Andrews, C., Nakazato, H., Oikawa, S., and Jessup, J.M. (1995). The effect of transfection of the CEA gene on the metastatic behavior of the human colorectal cancer cell line MIP-101. Cancer Lett *92*, 59-66.